International Journal of Thermophysics, Vol. 23, No. 1, January 2002 (© 2002)

Chain Dimensions in Polysilicate-Filled Poly(Dimethyl Siloxane)[1]

A. I. Nakatani,[2] W. Chen,[3] R. G. Schmidt,[3] G. V. Gordon,[3] and C. C. Han[2, 4]

Experimental results on the single-chain dimensions of isotopic blends (both mismatched and matched molecular masses) of poly(dimethyl siloxane) containing trimethylsilyl-treated polysilicate particles (fillers) are presented and compared with Monte Carlo calculations. For polymer chains that are approximately the same size as the filler particle, a decrease in chain dimensions is observed relative to the unfilled chain dimensions at all filler concentrations. For larger chains, at low filler concentrations, an increase in chain dimensions relative to the unfilled chain dimensions is observed. Both results are in agreement with existing Monte Carlo predictions. However, at even higher filler contents, which are beyond the scope of the Monte Carlo predictions, the chain dimensions reach a maximum value before decreasing to values which are still larger than the unfilled chain dimensions. A simple excluded volume model is proposed which accounts for these observations at higher filler content.

KEY WORDS: filled polymers; poly(dimethyl siloxane); polysilicate fillers; radius of gyration; small-angle neutron scattering.

1. INTRODUCTION

Filled polymers constitute a major portion of the commercial polymer market, and in most cases, fillers are used as economical additives for altering the mechanical behavior of polymers. In spite of widespread use, a fundamental understanding of how fillers modify mechanical behavior has

[1] Paper presented at the Fourteenth Symposium on Thermophysical Properties, June 25–30, 2000, Boulder, Colorado, U.S.A.

[2] National Institute of Standards and Technology, Polymers Division, Gaithersburg, Maryland 20899, U.S.A.

[3] Dow Corning Corporation, Midland, Michigan 48686, U.S.A.

[4] To whom correspondence should be addressed. E-mail: charles.han@nist.gov

0195-928X/02/0100-0199/0 © 2002 Plenum Publishing Corporation

not been achieved andachieved. While some researchers have attempted a rigorous approach toward understanding mechanical behavior in filled polymers [1–3], empirical relationships have dominated the field. Although these empiricisms have some predictive value, the underlying physical behavior of fillers in polymers is not understood. One need in the area of filled polymers is a molecular theory of elasticity, analogous to kinetic theories of rubber elasticity. One potential reason for the lack of such a theory is the scarcity of data available for filled polymers on fundamental quantities such as the radius of gyration. Mark and Curro have developed a theory of rubberlike elasticity, which accounts for non-Gaussian probability distributions of chains between cross-links [4, 5]. Mark and co-workers [6, 7] have used Monte Carlo techniques to calculate the distribution of polymer chain dimensions in the presence of filler particles. These theoretical, non-Gaussian distributions have been applied to the Mark and Curro theory to predict the stress–strain behavior and modulus of filled polymers. To our knowledge, experimental determination of the single-chain dimensions of a polymer in the presence of a filler particle has not been performed.

Small-angle neutron scattering (SANS) has been used to extract dimensions of polymer chains in multicomponent mixtures. For filled polymer systems, studies involving a number of different scattering techniques have been reported by other investigators [8–18]. These studies have focused on the structure and nature of the filler particles. Akcasu et al. [19] and Williams et al. [20] provided a framework for extracting single-chain structure factors from SANS measurements on multicomponent mixtures by the so-called high concentration method. Based on this earlier work, Summerfield and co-workers [21, 22] and King, Ullman, and co-workers [23, 24] derived a relationship for a three-component mixture of labeled and unlabeled polymers of matched molecular mass [25] and solvent. This method uses fixed compositions of solvent and total polymer (labeled and unlabeled) and varies the ratio of labeled-to-unlabeled polymer in the sample. By subtracting the appropriately weighted scattering intensities from samples with different labeling ratios, the single-chain structure factor of the polymers can be obtained. Because of the assumption of matched molecular masses of the polymers, one single-chain form factor is obtained for both the labeled and the unlabeled polymer. Tangari, Summerfield, and co-workers [26–28] examined the effects of mismatched molecular masses on the high concentration method. However, the presence of a third component was not considered in their treatment. The result is analogous to the result for isotopic blends with matched molecular masses except the single-chain form factor is the weighted sum of the individual form factors for the deuterated and protonated polymer chains. The primary assumption in the approach of Tangari and co-workers is that the

system is noninteracting. This assumption helps to eliminate a number of cross terms in the final expression for the total scattering intensity.

In this work, we present experimental results on the single-chain dimensions of isotopic blends (both mismatched and matched molecular masses) of poly(dimethyl siloxane) (PDMS) containing trimethylsilyl-treated polysilicate particles (fillers) and compare these results with the Monte Carlo calculations of Mark and co-workers. Our principal assumption is that the polysilicate filler may be effectively treated as a solvent molecule. The assumption that the polysilicate can be treated as a solvent molecule allows the analysis scheme of Tangari and co-workers to be combined with the results of Summerfield, King, Ullman, and co-workers to give the following expression for the scattering intensity:

$$I(q,\rho) = (a_H - a_D)^2\,\rho(1-\rho)[\rho S_S^H(q) + (1-\rho)\,S_S^D(q)] + [a_H(1-\rho) + a_D\rho - a_s']^2\,S_T(q) \tag{1}$$

where a_H, a_D, and a_s' are the monomer scattering lengths for the protonated polymer, deuterated polymer, and solvent, respectively, ρ is the fraction of deuterated polymer, $S_S^H(q)$ and $S_S^D(q)$ are the single-chain form factors for the protonated and deuterated polymers, respectively, and $S_T(q)$ is the interchain form factor. The magnitude of the scattering vector is defined as $q = (4\pi/\lambda)\sin(\theta/2)$, where θ is the scattering angle and λ is the incident wavelength. Equation (1) is the basis for extracting the chain dimensions in this study. From the single-chain form factors, $S_S^i(q)$, R_g may be calculated as follows:

$$1/S_S^i(q) = \text{const.}\,(1 + q^2R_g^2/3) \tag{2}$$

where $R_g = \sqrt{N_i b^2/6}$, N_i is the degree of polymerization of the polymer, and b is the polymer statistical segment length, yielding the R_g of the polymer chains.

For comparison, the radii in the unfilled, isotopic blends were examined as a function of the ratio of labeled-to-unlabeled polymer. The results for the isotopic blends were analyzed using the two-component random phase approximation (RPA) theory [29]:

$$S(q) = k_N\{[\phi_A v_A N_A g_D(x_A)]^{-1} + [\phi_B v_B N_B g_D(x_B)]^{-1} + (2\chi/v_0)\}^{-1} + \text{Baseline} \tag{3}$$

where N_i is the degree of polymerization index, ϕ_i is the volume fraction, v_i is the molar volume of the ith component, v_0 is a reference volume, and k_N is the contrast factor:

$$k_N = N_0[(a_A/v_A)-(a_B/v_B)]^2 \tag{4}$$

In Eq. (4), N_0, a_i, and v_i are, respectively, Avogadro's number, the scattering length, and the molar volume of a monomer unit of the ith component. For polydisperse materials, in Eq. (3), the N_i are replaced by $\langle N_i\rangle_n$, the number-average degree of polymerization, and the Debye functions, $g_D(x_i)$ are replaced by the mass average Debye function given by Eq. (5), assuming a Schultz–Zimm distribution for the molecular masses:

$$\langle g_D(x_i)\rangle_w = (2/x_i^2)\{x_i - 1 + [h/(h+x_i)]\,h\} \tag{5}$$

where $x_i = q^2\langle N_i\rangle_n\, b^2/6$, $h = [\langle N_i\rangle_w/\langle N_i\rangle_n - 1]^{-1}$ and $\langle N_i\rangle_w$ is the mass-average degree of polymerization. By fitting the isotopic blend data to Eq. (3), the parameters b, χ/v_0, and the incoherent baseline are obtained. The value of b is an average value for both of the polymers. Based on the values for $\langle N_i\rangle_w$ obtained by size-exclusion chromatography (SEC) for each polymer, the R_g of each polymer is obtained ($R_g = (\langle N_i\rangle_w\, b^2/6)^{1/2}$).

2. EXPERIMENTAL

2.1. Materials

The PDMS polymers (density = 0.97 $g\cdot cm^{-3}$) were provided by Dow Corning Corporation [30]. Deuterated PDMS (d-PDMS) was synthesized via the hydrolysis and condensation of perdeuterated chlorosilanes. The molecular masses were characterized independently by SEC using PDMS standards. Four polymers (Table I) were available for this study and were designated 100DP h-PDMS, 100DP d-PDMS, 1000DP h-PDMS, and 1000DP d-PDMS. The mismatch in molecular mass between the 100DP h-PDMS and the 100DP d-PDMS necessitated the application of the data analysis scheme for mismatched molecular mass polymers in solvent described above.

The trimethylsilyl-treated polysilicate material (density = 1.05 $g\cdot cm^{-3}$, M_n = 1500 $g\cdot mol^{-1}$ by SEC) was synthesized via the cohydrolysis and condensation of hexamethylsiloxane and a tetraalkoxysilane (mole ratio = 1.2:1), giving a final composition of $(Me_3SiO_{1/2})_{0.54}(HOSiO_{3/2})_{0.02}(EtOSiO_{3/2})_{0.03}(SiO_{4/2})_{0.41}$ (subscripts indicate mass fractions of each structural unit). The trimethylsilyl treatment of the polysilicate renders the particle surface nonreactive, thereby enhancing the particle size stability and improving the

Table I. Homopolymer Characteristics[a]

Polymer	M_0	M_w(SEC)	M_w/M_n(SEC)	DP_w	M_w(Zimm)	R_g (Å)	A_2 (mol·cm^3·g^{-2})
100DP h-PDMS	74	12.0×10^3	1.05	160	15.8×10^3 $\pm1.0\times10^3$	33.6 ±1.0	6.92×10^{-4} $\pm0.50\times10^{-4}$
100DP d-PDMS	80	38.1×10^3	2.50	476	34.7×10^3 $\pm6.0\times10^3$	76.5 ±5.0	5.20×10^{-4} $\pm0.70\times10^{-4}$
1000DP h-PDMS	74	85.7×10^3	3.82	1160	89.9×10^3 $\pm15.0\times10^3$	110.0 ±5.0	5.50×10^{-4} $\pm0.40\times10^{-4}$
1000DP d-PDMS	80	81.7×10^3	4.16	1021	85.4×10^3 $\pm8.0\times10^3$	114.1 ±7.0	3.10×10^{-4} $\pm0.60\times10^{-4}$
Polysilicate filler	72	1.9×10^3[b]	1.23	26	5.7×10^3 $\pm1.0\times10^3$	10.6 ±1.5	3.47×10^{-3} $\pm0.38\times10^{-3}$

[a] M_0, M_w, and M_n are the monomer, mass average, and number-average molecular masses, respectively, in g·mol^{-1}. DP_w is the mass average degree of polymerization obtained from M_w(SEC), and R_g is the radius of gyration obtained from dilute solution SANS measurements.

[b] M_n obtained from SEC. A_2 values are for the polymer in toluene (toluene-d_8 for protonated samples, toluene-h_8 for deuterated samples). ± values for Zimm M_w, R_g, and A_2 are derived from standard error estimates of the slope and intercept values from linear regression fits to the extrapolated $c=0$ and $q=0$ lines of Zimm plots.

compatibility of the filler with the PDMS. The polysilicate material has a nonlinear, amorphous, particulate structure. At low temperatures these materials exhibit glassy behavior but display a rapid decrease in modulus near their effective glass transition temperature (T_g) of -70°C (as determined by dynamic mechanical thermal analysis). Since the molar mass of the polysilicate filler is relatively low and the structure is compact, the filler does not exhibit any signs of molecular entanglement during the transition from a glassy to a liquid material near T_g. Introduction of the polysilicate to linear PDMS results in a slight increase in T_g of the PDMS and a reduction in the crystallization of the PDMS.

2.2. Small-Angle Neutron Scattering

SANS measurements were carried out at the Cold Neutron Research Facility of the NIST Center for Neutron Research. Data were collected on the 8-m SANS instrument with the neutron wavelength, $\lambda=12.0$ Å, and a sample-to-detector distance of 3.6 m, giving a q range of 0.008 to 0.065 Å^{-1}. The samples were either placed 1-mm-pathlength quartz cells (100DP blends) or sandwiched between quartz windows with a 0.5-mm spacer

(1000DP blends). All samples were prepared by weighing the appropriate amounts of each component in a screw-top vial and placing the vials on a roller (roller speed, ca. 1 rpm) for 24 h at ambient temperature to mix the samples mechanically. Data were collected over a two-dimensional detector and corrected for dark current intensity due to electronic and background neutron noise and empty cell scattering. Background scattering, due mainly to incoherent scattering, of the protonated components (both the protonated PDMS and the polysilicate filler) in the samples was also subtracted separately during the data reduction. Absolute intensity calibration used a dry silica gel as a secondary standard, calibrated in terms of a primary vanadium standard.

3. RESULTS

The scattering from the 100DP and 1000DP isotopic blends without filler was measured and analyzed by fitting the experimental data to the RPA equation [Eq. (3)] using a nonlinear least-squares regression routine. Different ratios of deuterated-to-protonated polymer were prepared to examine the composition dependence of R_g for each isotopic blend. The χ/v_0 values are close to zero (ca. -10^{-5} to -10^{-6} mol·cm^{-3}), while the calculated values for χ/v_0 at the spinodal temperature are of the order of 0.01 mol·cm^{-3}. This indicates that these blends are far from phase separating, and the experiments were conducted well into the miscible region of the phase diagram. We noted no systematic variation of χ/v_0 or b between 30 and 90°C, which also indicates that the blends are completely miscible.

Some unanticipated concentration dependence of R_g and the associated parameters, χ/v_0 and b, was observed in the isotopic blends. While the discussion of this behavior is beyond the scope of this paper, the presence of this concentration dependence in R_g complicates the determination of the unfilled chain dimensions. Only a range of unfilled R_g values can be compared to the filled R_g values, since the experiments on the three-component mixtures were performed at fixed ratios of total polymer to filler with varying ratios of labeled-to-unlabeled polymer. Significant changes in the chain dimensions in the presence of filler are harder to assess because of this concentration dependence in R_g.

For the filled 100DP mixtures, five ratios of labeled-to-unlabeled chains were examined. For the solution to three linear equations and three unknowns, these five different labeling ratios provide 10 solutions for each of the three unknowns (S_S^H, S_S^D, and S_T). Due to the polydispersity of the 1000DP samples, six labeling ratios were measured for most concentrations of the filler. This allowed us to obtain 20 solutions to the system of linear

equations. As expected for polymers of different molecular mass, the single-chain form factors for the 100DP polymers are distinct, while the single-chain form factors for the 1000DP polymers of matched molecular mass are similar. For all filler concentrations, the results presented below are the mean values obtained from all of the physically realistic solutions to the systems of linear equations.

The solutions to the systems of linear equations were used to construct plots of $1/S_S^i$ against q^2. Linear fits to Eq. (2) were used to obtain the R_g values. The fit range for the 100DP samples was $0.015\ \text{Å}^{-1} < q < 0.060\ \text{Å}^{-1}$ and the range for the 1000DP samples was $0.010\ \text{Å}^{-1} < q < 0.040\ \text{Å}^{-1}$. These q ranges do not completely satisfy the necessary condition, $qR_g < 1$. Ullman [31] has analyzed the errors when this condition is not satisfied and estimates errors as large as 20% are possible. By fitting the data over a consistent q range, we believe that the relative variation in R_g values is correct. The reported R_g values are the means obtained from all the linear fits at each filler concentration.

The variation in R_g as a function of filler concentration is shown in Figs. 1 and 2 for the 100DP blend and 1000DP blend, respectively. The vertical bars on the data points represent ± 1 standard deviation, and the

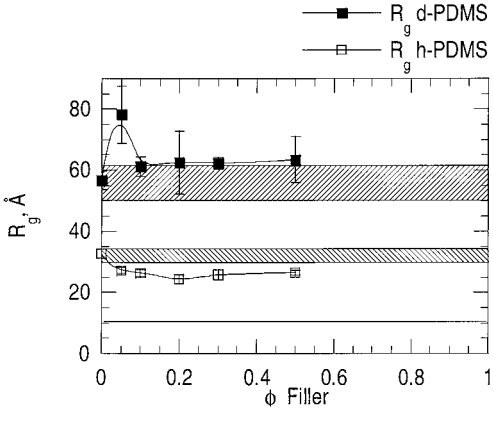

Fig. 1. Apparent R_g values of 100DP d-PDMS and 100DP h-PDMS as a function of polysilicate filler concentration. Bars in figures represent ± 1 standard deviation in the measurements assuming normal, random statistical errors. Solid line indicates the R_g value for the polysilicate. Crosshatched areas indicate the range of R_g values for each component in the unfilled blend obtained from the RPA analysis. (////) h-PDMS R_g range; (\\\\) d-PDMS R_g range.

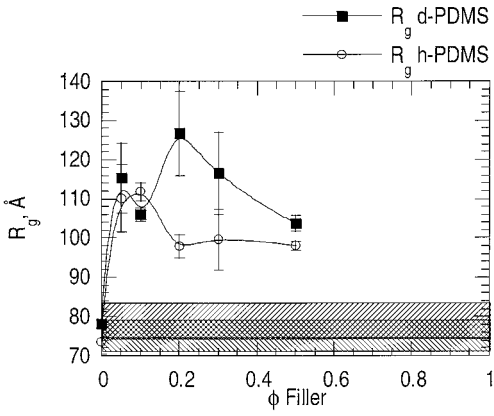

Fig. 2. Apparent R_g values of 1000DP d-PDMS and 1000DP h-PDMS as a function of polysilicate filler concentration. Bars in figures represent ± 1 standard deviation in the measurements assuming normal, random statistical errors. Crosshatched areas indicate the range of R_g values for each component in the unfilled blend obtained from the RPA analysis. (////) h-PDMS R_g range; (\\\\) d-PDMS R_g range.

solid lines represent smooth curve fits to the data as a guide to the eye. In each plot, the range of R_g values for the unfilled polymers obtained from the RPA fits are shown by the crosshatched areas. In Fig. 1, the R_g value of the filler is shown by the solid line at 10.6 Å. In the 100DP blend, the 100DP h-PDMS shows a slight decrease in R_g with increasing filler concentration. This decrease appears to be significant since all values and the associated errors lie below the range of unfilled R_g values. The 100DP d-PDMS shows much different behavior. The value of R_g first increases drastically at low filler content (mass fraction of 5%), then decreases to values which appear to be slightly larger than the unfilled R_g. However, the standard errors on the values for the 100DP d-PDMS are much larger than for the 100DP h-PDMS, therefore, beyond the initial increase in chain dimensions at 5% filler, the chain dimensions at higher filler contents are statistically the same as the unfilled chain dimensions.

In Fig. 2, both the 1000DP h-PDMS and the 1000DP d-PDMS R_g values behave similarly as a function of filler concentration. The behavior is also similar to the behavior of the 100DP d-PDMS described above. At low filler contents, the R_g values of both the h- and the d-PDMS increase and then decrease at higher concentrations. However, the R_g values at higher filler contents are significantly greater than the unfilled chain dimensions.

While the general behavior of both polymers is similar, there are slight differences between the h-PDMS and the d-PDMS. For the 1000DP h-PDMS, the maximum R_g value occurs around a filler content of 10%, whereas the maximum R_g value for the 1000DP d-PDMS occurs at a filler concentration of 20%. The R_g values for the 1000DP h-PDMS above a 20% filler concentration are all approximately the same, while the R_g values for the d-PDMS decrease gradually between filler concentrations of 20 and 50%.

4. DISCUSSION

The SANS determination of R_g as a function of filler content has a qualitative resemblance to the Monte Carlo calculations of chain dimensions in the presence of spherical particles by Mark and co-workers. Yuan et al. [7] examined PDMS chains mixed with silica filler particles by adopting a rotational isomeric state model for the PDMS and assuming no interactions between the filler and the chain. For the cases where the polymer chains were much larger than the filler particles, the size of the chains increased with increasing filler concentration. However, for a polymer with dimensions approaching the size of the filler particles, the size of the chains decreased slightly with increasing filler concentration.

Although the assumptions that our fillers can be treated as a solvent molecule and that all components are noninteracting may not be rigorously correct, the polymer R_g values obtained in the filled samples appear to be reasonable. For the polymer with chain dimensions approaching the dimensions of the filler (100DP h-PDMS), the decrease in chain dimensions with increasing filler content is similar in magnitude to the change predicted by the Monte Carlo calculations. For the cases where the polymer chain dimension is larger than the filler particle, Yuan et al. [7] performed calculations to filler concentrations of 10% compared to our samples containing up to 50% filler. While the Monte Carlo calculations for polymer chains much larger than the filler particles showed a monotonic increase in the chain dimensions in the filled samples with increasing filler content, our results (Figs. 1 and 2) indicate that the chain dimensions reach a maximum at low filler contents, then decrease at higher filler concentrations. However, at all concentrations, the chain dimensions are greater than the unfilled chain dimensions.

An extension of the excluded volume model of Yuan et al. [7] may provide an explanation for our results. At sufficiently low filler concentrations, chain expansion is observed (Fig. 3a). However, if the concentration of small filler particles increases to the point where they begin to touch and interconnect (Fig. 3b), a large portion of the volume defined at the start of the calculation is unavailable to the chain, and the chain dimensions

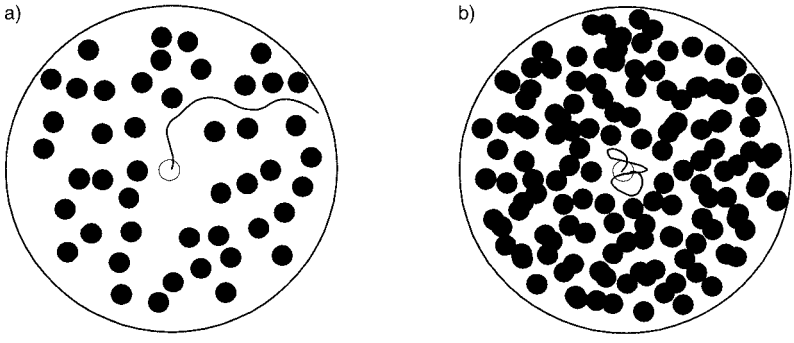

Fig. 3. Proposed model for chain behavior in the presence of filler for chains much larger than the filler particle: (a) at low concentrations (chain expansion); (b) at high filler concentrations (chain collapse).

decrease. Further Monte Carlo calculations to test this hypothesis would be desirable. Similar measurements on larger polysilicate fillers and more traditional fumed silicas as a function of the particle size and concentration and measurements on filled, cross-linked systems as a function of deformation could both provide the necessary molecular level information for comparison to a molecular theory of elasticity.

ACKNOWLEDGMENTS

We wish to acknowledge discussions with Drs. B. J. Bauer and B. Hammouda of NIST and Dr. A. Z. Akcasu of the University of Michigan concerning the data treatment for the three-component mixtures. The preparation and purification of deuterated siloxane monomers and polymerization were completed by A. P. Wright, B. Zhong, T. M. Leaym, G. M. Wieber, and R. G. Taylor of Dow Corning and greatly appreciated.

REFERENCES

1. M. Kluppel and G. Heinrich, *Rubber Chem. Tech.* **68**:623 (1995).
2. G. Heinrich and T. A. Vilgis, *Macromolecules* **26**:1109 (1993).
3. T. A. Witten, M. Rubinstein, and R. H. Colby, *J. Phys. II France* **3**:367 (1993).
4. J. E. Mark and J. G. Curro, *J. Chem. Phys.* **79**:5705 (1983).
5. J. G. Curro and J. E. Mark, *J. Chem. Phys.* **80**:4521 (1984).
6. A. Kloczkowski, M. A. Sharaf, and J. E. Mark, *Chem. Eng. Sci.* **49**:2889 (1994).
7. Q. W. Yuan, A. Kloczkowski, J. E. Mark, and M. A. Sharaf, *J. Polym. Sci. Polym. Phys. Ed.* **34**:1647 (1996).
8. P. Bezot, C. Hesse-Bezot, B. Rousset, and C. Diraison, *Colloids Surfaces A* **97**:53 (1995).
9. P. W. Schmidt, *J. Appl. Cryst.* **15**:567 (1982).

10. R. J. Young, D. H. A. Al-Khudhairy, and A. G. Thomas, *J. Mater. Sci.* **21**:1211 (1986).
11. L. Karásek and M. Sumita, *J. Mater. Sci.* **31**:281 (1996).
12. T. Freltoft, J. K. Kjems, and S. K. Sinha, *Phys. Rev. B* **33**:269 (1986).
13. G. D. Wignall, N. R. Farrar, and S. Morris, *J. Mater. Sci.* **25**:69 (1990).
14. L. Salome and F. Carmona, *Carbon* **29**:599 (1991).
15. R. P. Hjelm, P. A. Seeger, and W. A. Wampler, *Polym. Polym. Comp.* **1**:53 (1993).
16. L. Salomé, *J. Phys. II France* **3**:1647 (1993).
17. R. P. Hjelm, W. A. Wampler, P. A. Seeger, and M. Gerspacher, *J. Mater. Res.* **9**:3210 (1994).
18. D. W. M. Marr, M. Wartenberg, K. B. Schwartz, M. M. Agamalian, and G. D. Wignall, *Macromolecules* **30**:2120 (1997).
19. A. Z. Akcasu, G. C. Summerfield, S. N. Jahshan, C. C. Han, C. Y. Kim, and H. Yu, *J. Polym. Sci. Polym. Phys. Ed.* **18**:863 (1980).
20. C. E. Williams, M. Nierlich, J. P. Cotton, G. Jannink, F. Boué, M. Daoud, B. Farnoux, C. Picot, P. G. deGennes, M. Rinaudo, M. Moan, and C. Wolff, *J. Polym. Sci. Polym. Lett. Ed.* **17**:379 (1979).
21. S. N. Jahshan and G. C. Summerfield, *J. Polym. Sci. Polym. Phys. Ed.* **18**:1859 (1980).
22. S. N. Jahshan and G. C. Summerfield, *J. Polym. Sci. Polym. Phys. Ed.* **18**:2415 (1980).
23. J. S. King, W. Boyer, G. D. Wignall, and R. Ullman, *Macromolecules* **18**:709 (1985).
24. R. Ullman, H. Benoit, and J. S. King, *Macromolecules* **19**:183 (1986).
25. According to ISO 31-8, The term "molecular mass" has been replaced by "relative molecular mass," symbol M_r. Thus, if this nomenclature and notation were to be followed, one would write, $M_{r,n}$, instead of the historically conventional M_n for the number average molecular weight and it would be called the "number-average relative molecular mass." The conventional notation, rather than the ISO notation, has been employed for this publication.
26. C. Tangari, G. C. Summerfield, J. S. King, R. Berliner, and D. F. R. Mildner, *Macromolecules* **13**:1546 (1980).
27. G. C. Summerfield, *J. Polym. Sci. Polym. Phys. Ed.* **19**:1011 (1981).
28. C. Tangari, J. S. King and G. C. Summerfield, *Macromolecules* **15**:132 (1982).
29. P. G. de Gennes, *Scaling Concepts in Polymer Physics* (Cornell University Press, Ithaca, NY, 1979).
30. Certain equipment and instruments or materials are identified in this paper to specify the experimental details adequately. Such identification does not imply recommendation by the National Institute of Standards and Technology, nor does it imply that the materials are the best available for the purpose.
31. R. Ullman, *J. Polym. Sci. Part B: Polym. Phys. Ed.* **23**:1477 (1985).